Journal of Hand Surgery Global Online 4 (2022) 135–140

Contents lists available at ScienceDirect

Journal of Hand Surgery Global Online

journal homepage: www.JHSGO.org

Original Research

Appropriately Matched Fixed-Angle Locking Plates Improve Stability in Volar Distal Radius Fixation

Natalia D. McIver, MS, * Christina Salas, PhD, * Nathan Menon, MD, * John Heifner, MD, † Deana Mercer, MD *

* Department of Orthopaedics & Rehabilitation, the University of New Mexico Health Sciences Center, Albuquerque, NM
† St George's University School of Medicine, Great River, NY

ARTICLE INFO

Article history:
Received for publication November 22, 2021
Accepted in revised form February 16, 2022
Available online April 4, 2022

Key words:
Distal radius fracture
Distal radius morphology
Fixed-angle volar locking plate
Volar fixation
Volar locking plate

Purpose: Size options for volar locking plates may provide value for distal radius fixation. We compared excessively narrow plates with plates that were appropriately matched in width for fixation of an multifragmented distal radius fracture model.
Methods: Eighteen matched pairs (right and left wrists) of large, cadaveric male distal radii specimens, prepared with a simulated Arbeitsgemeinschaft für Osteosynthesefragen type C-3 distal radius fractures, were tested. One specimen from each matched pair was randomized to receive a plate that was appropriately matched in width to the distal radius. The contralateral limb received a narrow plate, which in all cases was undersized in width. Fixation stability was tested and compared to the contralateral matched specimen. Specimens were preloaded at 50 N for 30 seconds before cyclic loading from 50–250 N at 1 Hz for 5000 cycles then loaded to failure.
Results: Loss of fixation under cyclic loading was significantly greater in the specimens fixed with excessively narrow plates compared with plates of appropriate width. When loaded to failure, the plates of appropriate width were stiffer, with higher force at failure and compressive strength than narrow plates. The primary mode of failure was displacement of the distal lunate facet fragment.
Conclusions: These findings suggest that optimally matching the volar locking plate width to the radius may provide advantages for stability of the fixation construct and fragment capture. This may be due to reduced stress concentration from the distribution of forces across a larger surface area.
Clinical relevance: Optimizing the plate width to the radial width may improve fracture stability and may carry additional importance in comminuted fractures, where narrow plates may not completely capture small bone fragments.

Volar locked plating has become the most common surgical fixation method used for distal radius fractures.[1] Advantages of volar locked plating include the ability to address a wide spectrum of fracture morphology and the ability to neutralize forces across the fracture site, allowing for early motion.[2–4] These factors have contributed to the recent improvement in patient outcomes, compared with historical reports using other forms of fixation.[5]

Early motion substantially improves pain and function in the months after volar fixation of the distal radius.[6] Therefore, the fixation construct must withstand the forces applied during this rehabilitation period. Forces induced across the fracture in the early rehabilitation period can be significant. For every 8 Newtons of handgrip force, 22 to 48 Newtons of force is produced across the wrist and through the distal radius.[7] Hence, volar plates should confer sufficient stability in order to perform the activities of daily living. These requirements may be amplified in complex, multifragmentary fractures, where stability is more challenging to maintain.

Because of the variability of the distal radius anatomy, size options are available for volar locking plates, and they provide value for restoring the anatomy.[8,9] The plate position and plate size

Declaration of interests: D.M. discloses speaker's bureau for Skeletal Dynamics and Axogen. No benefits in any form have been received or will be received by the other authors related directly or indirectly to the subject of this article.

Corresponding Author: Deana Mercer, MD, Department of Orthopaedics and Rehabilitation, University of New Mexico, MSC10 5600, Albuquerque, NM 87131.
E-mail address: dmercer@salud.unm.edu (D. Mercer).

https://doi.org/10.1016/j.jhsg.2022.02.007

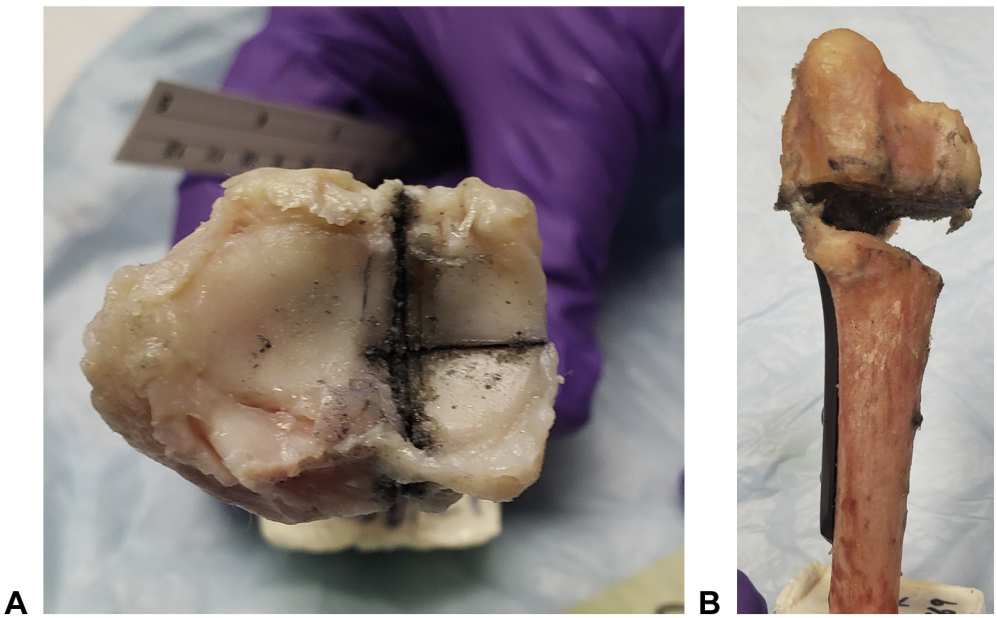

Figure 1. Simulated Arbeitsgemeinschaft für Osteosynthesefragen type C-2 multifragmentary articular fracture. **A** Axial view showing 3 fragments. **B** Lateral view showing the 1-cm extra-articular osteotomy positioned 1.5 cm from the distal articular surface.

play a critical role, imparting stability and ensuring adequate subchondral support.[5,8,10–12] Plates that are too small may provide inadequate coverage, which can weaken the fixation.[11] Plates that are too large can lead to soft-tissue irritation and subsequent plate removal because of pain. There is a potential for surgeons to choose smaller plates than those optimally matched to the size of the radius, because smaller plates are easier to apply and more forgiving to slight imperfections in placement or reduction.[13,14] Although volar plate size has been qualitatively discussed in reference to stability, determining the comparative stability between plate sizes would improve understanding and provide clinically relevant information.

We conducted an experiment to compare an excessively narrow plate with a plate that was appropriately matched in width for fixation of a complex, multifragmented distal radius fracture. We tested loss of fixation under cyclic loading, stability of the fracture construct under static loading, load to failure, compressive strength of the fixation construct, volar width spanned by the plate, and volar surface area coverage. We hypothesized that the appropriately matched plates would demonstrate superior results.

Materials and Methods

Specimen preparation

A prestudy power analysis of 6 matched pairs of specimens showed that a minimum sample size of 15 matched pairs would be needed to observe a statistical difference in outcomes at a 5% level of significance. We used 18 male, matched pairs of fresh-frozen human cadaver forearms (n = 36; mean age, 57 years; and mean weight, 261.9 pounds). Heavier male specimens were chosen to increase the probability of the specimen being adequately sized for our study. This reduces the potential for methodological bias because of a standard or wide plate being too large for the specimen. Specimens were thawed for 24 hours, and computed tomography scans were taken with a calibration phantom positioned in the field of view for subsequent analysis and morphometric measurements. Materialise Interactive Medical Image Control System (Materialise) was used to segment the distal radii from the surrounding soft tissue. The cross-sectional area of the bones was calculated at a position 1.5 cm from the distal articular surface. Specimens were refrozen until 24 hours before the day of testing, at which time the distal radii were dissected.[15] Each radial shaft was cut to the same length, pinned proximally with K-wires, and potted with urethane casting resin (Smooth-Cast 300, Smooth-On Inc) for securing the radii to the test fixture.

An Arbeitsgemeinschaft für Osteosynthesefragen type C-3 multifragmentary articular fracture was simulated on each radius by removing a 1-cm segment of bone with the apex 1.5 cm proximal to the distal articular surface. Three articular fragments were generated by making a sagittal cut, separating the scaphoid and lunate facets, followed by a coronal cut of the lunate fragment (Fig. 1). One specimen from each pair was randomized to the appropriately matched plate group, where a wide plate or a standard plate was always found to be the optimal fit. Differences between standard and wide plates were not assessed. Specimens in the appropriately matched plate group received either a standard or a wide plate but never a narrow plate, because it was never found to be optimal for these large specimens. The contralateral radius always received a narrow plate. A controlled randomization procedure was used to ensure an equivalent number of left and right limbs in each test group.

Implant placement

Narrow, standard, and wide Geminus (Skeletal Dynamics) volar distal radius plates with 4 diaphyseal screw holes were used, which all use a dual-column design to support each fossa independently. Multiplanar distal fixed-angle screws are used for subchondral bone support. The narrow, standard, and wide plates measure 21.1 mm, 24.4 mm, and 26.4 mm in width, respectively. Narrow plates offer 3 fixation points in the intermediate or lunate fossa column. Standard or wide plates offer 4 fixation points in the intermediate or lunate fossa column. The appropriately matched plate group had

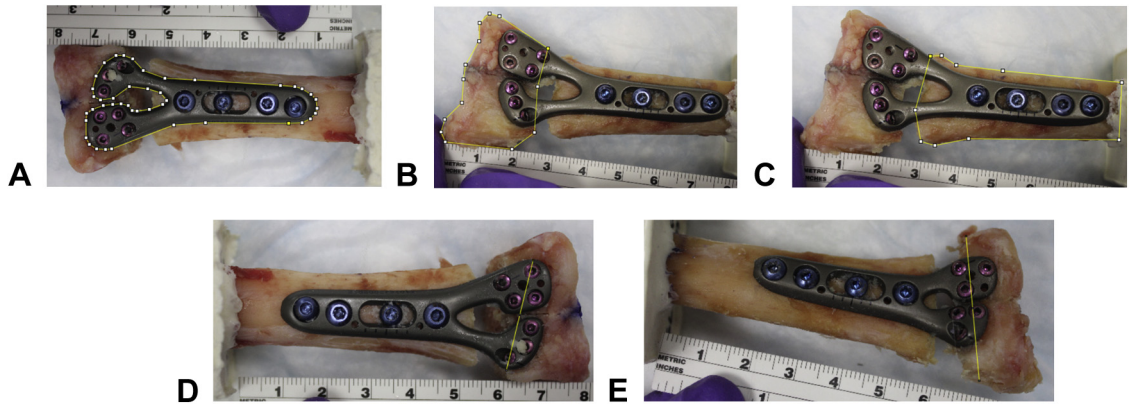

Figure 2. Prestudy image analysis was completed using ImageJ to analyze the percentage of plate surface area coverage on bone **A**–**C** and plate-to-bone percentage width **D**–**E**. **A** Image analysis of plate surface area. **B** Distal and **C** proximal volar surface area analysis. **D** Plate width analysis at the longest width of the plate. **E** Bone width analysis at the widest location of the distal fragment covered by the plate.

a plate width that most closely matched the width of the distal radius without exceeding its transverse bony dimension. All the specimens in the appropriately matched group received either a standard or a wide plate. The technique used for plate implantation was uniform for both groups. The distal edge of the plate was placed approximately 2 mm proximal to the watershed line, with the proximal end of the plate aligned with the radial shaft. A nonlocking screw was first placed in the shaft gliding hole. We first reduced the lunate facet fragment, followed by the scaphoid facet fragment, which was stabilized with a K-wire. Fluoroscopy was used to confirm the K-wire placement, fracture reduction, and screw length on an extended tangential view.[16] Screw lengths in the articular segment were implanted 2 mm shorter than the measured length. The remainder of the distal and shaft screws were placed by first predrilling the hole, then measuring the length, and then placing the screw.

Prestudy image analysis

Before testing, photographs were taken of the specimens, with implants fixed to the volar surface. A soft surgical ruler was placed in the field of view at the level of the bone-implant interface for calibration of each specimen. ImageJ software (National Institute of Health, Bethesda, Maryland, USA) was used to take 4 measurements, including the volar surface area of the radius, the surface area of the plate, the width of the distal radius at its widest cross-section, and the width of the plate at the location of the widest cross-section of the distal radius (Fig. 2).[17]

Experimental testing

A Mini Bionix servohydraulic load frame and a 15 kN load cell were used for testing (MTS Systems). The proximal potted block was fixed to the actuator in line with the radial shaft. An angled vise and custom fixture allowed a load ratio of 60% to 40% to be applied to the scaphoid and lunate facets, respectively.[18] Specimens were preloaded to 50 N for 30 seconds, then sinusoidally compressed from 50 to 250 N at 1 Hz for 5,000 cycles to simulate light, active weight bearing, as would be prescribed by the surgeon during the immediate postoperative period.[3] Similar loading parameters have been commonly used in biomechanical studies of volar locked plates (VLPs).[19–23]

Specimens were then subjected to a ramped load until failure at a rate of 1 mm/s, simulating a fall on an outstretched hand. Video was captured of the failure event, and postfailure images were taken.

Outcome measures and statistical analysis

Cyclic

Outcome measures included a loss of fixation during cyclic loading, as measured by the difference in displacement between cycle 5 and cycle 5,000 at the 250 N compression threshold when comparing the plate size groups. Cycle 5 was chosen as the initial cycle, because it was the point at which settling of the bone-implant fixture was no longer observed in the data.

Load to failure

Outcome measures included the stiffness of bone-implant constructs (slope of the most linear region of the force and displacement curve), ultimate force at failure, and ultimate compressive strength of the bone-implant construct. We report the percentage of the volar surface area covered by the plate and the percentage of the radial width spanned by the plate to ascertain whether any experimental findings may be a function of plate size. We also report the mode of failure for all specimens.

Statistical analysis

Cyclic and failure data analyses were completed with the use of MATLAB software (MathWorks). A 1-tailed, matched-pair *t* test was used to determine the statistical significance at an alpha level of 0.05 between the plate size groups.

Results

During a simulated postoperative cyclic loading period, loss of fixation was significantly greater in the specimens treated with narrow plates (0.75 ± 0.31 mm) than that in the specimens treated with appropriately matched plates (0.63 ± 0.15 mm; P = .05). A representative example of the force-displacement hysteresis curves during cyclic loading for 1 specimen pair is shown in Figure 3.

In a simulated failure-loading scenario, the specimens treated with appropriately matched plates (529.4 ± 113.0 N/mm) were significantly stiffer than the specimens treated with narrow plates (396.3 ± 131.5 N/mm; P = .01) (Table 1). The specimens treated with appropriately matched plates (1101.7 ± 199.8 N) had a higher ultimate force prior to failure than the specimens treated with narrow plates (852.3 ± 120.6 N). For ultimate force, the mean of the

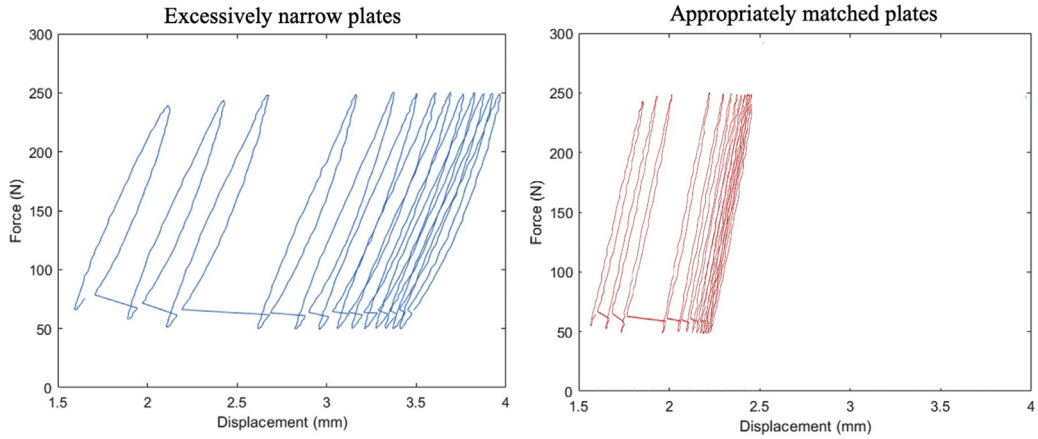

Figure 3. Representative force-displacement hysteresis curves showing a single specimen treated with a narrow plate (left) and an appropriately matched plate (right) during the 5,000-cycle test period.

differences was 249.4 N/mm ($P < .001$). The ultimate compressive strength was significantly higher for the specimens treated with appropriately matched plates (1.84 ± 0.4 MPa) than for the specimens treated with narrow plates (1.44 ± 0.3 MPa; $P < .001$).

Wide plates covered 52.9% of the surface area of the distal radius and spanned 85.3% of the width of the distal radius. Standard plates covered 49.4% of the surface area of the distal radius and spanned 81.3% of the width. Narrow plates covered only 39.0% of the surface area of the distal radius and spanned 63.3% of the width. The percentage of the plate coverage area had a moderate correlation to the ultimate force ($R^2 = 0.48$) and a moderate correlation to the ultimate compression strength ($R^2 = 0.45$).

There were 5 identifiable modes of failure in this study: (1) specimens failed by dorsal lunate facet fracture (n = 20), (2) extra-articular gap closure (n = 2), (3) complete lunate (volar and dorsal) facet fracture (n = 10), (4) scaphoid facet fracture only (n = 1), and (5) scaphoid and dorsal lunate facet fracture (n = 3). Representative images of these modes of failure can be seen in Figure 4.

Discussion

Perren[24] described stability as the lack of deformation of a fracture fixation construct under load. In a simulated weight-bearing scenario that may be comparable to early postoperative rehabilitation, our results demonstrated a significant difference in the stability of the fixation construct between narrow and appropriately matched plates. This suggests that appropriate plate sizing may play a role in construct stability within a clinically relevant load-bearing scenario. According to Putnam et al,[7] the load across the distal radius is 3–5 times the grip force. It is not unusual for patients to use their hands for activities of daily living early in the rehabilitation period. Simple tasks can generate great forces on the distal radius. For example, lifting a quart of milk may require a grip force of 10 N, which means the load on the distal radius may be up to 50 N. Therefore, the fixation must be able to tolerate these forces to provide the desired anatomical results.

Table 1
Stiffness and Load to Failure Results Comparing Volar Locking Plate Size in Articular Models of Distal Radius Fracture

	Appropriately Matched VLP	Excessively Narrow VLP
Stiffness ($P = .01$)	529.4 (±113 N/mm)	396.3 (±131.5 N/mm)
Load to failure ($P = .001$)	1101.7 (±199.8 N/m)	852.3 (±120.6 N/mm)

Stress is a function of force and the cross-sectional area. For a given radius, maximizing the articular surface area directly supported by the spread of the distal fixed-angle screws or pegs will lower stress concentration and, therefore, may improve fracture stability. Appropriately matching the plate width to the radius maximizes the number of fixation points for fragmentary capture and improved buttressing capacity, because smaller plates may have fewer fixation points. This is a direct result of the size of the area available on the distal plate to accommodate distal screws or pegs. An appropriately matched plate may be advantageous in comminuted fractures, where excessively narrow plates may not effectively capture all small fragments. Törnkvist et al[25] and others have described increased construct strength with a greater number of screws and a greater spacing of the screws.[26] Further, torsional strength is gained with an increasing number of screws. This has clinical applicability, because the degree of torsional forces produced by rehabilitation may also be substantial.[27]

The narrow plate used in this study contains 3 screws to support the subchondral region of the lunate facet, compared to the standard or wide plates that contain 4 screws in this region. When evaluating the mechanisms of failure in narrow plates, 89% were due to failure of the lunate facet fragment. It is possible that the reduced number of screws was insufficient to support the high loads that are transferred across this region in these larger specimens fixed with excessively narrow plates.

A potential complication from an undersized VLP is articular penetration into the scaphoid fossa by the radial styloid screw or peg. Applied articular loads push the joint surface onto the tip of the most radial screw or peg, creating a localized, high-stress concentration that can result in joint penetration. Plates that are appropriately matched in width place the tip of the most radial screw at or lateral to the radial styloid, as opposed to under the joint surface. In this setting, the shaft of the screw supports the subchondral bone of the scaphoid fossa, as opposed to the tip of the screw. This reduces the risk of articular penetration.

Complications may arise from oversized VLPs. Attention must be given to the plate size as well as the plate position. Coronal plane malposition has been associated with discomfort and subsequent plate removal.[14] The extent of the coronal plane width of the distal portion of the plate should not encroach on the cortical margins, and the proximal shaft of the plate should align colinearly with the longitudinal axis of the radius. Based on the current results, using the widest plate while respecting these criteria may provide improved stability and maximize subchondral support.

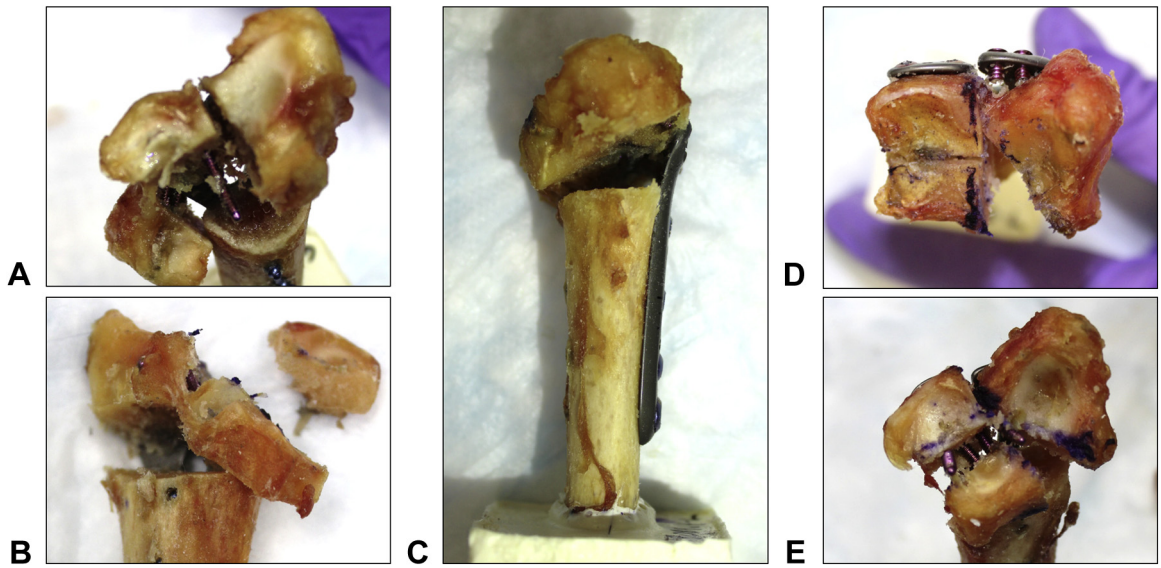

Figure 4. Images depicting the modes of failure for specimens. **A** dorsal lunate facet failure (n = 20); **B** complete lunate facet failure, dorsal and volar (n = 10); **C** extra-articular gap closure (n = 2); **D** scaphoid facet failure (n = 1); and **E** scaphoid and dorsal lunate facet failure (n = 3).

Limitations include those inherent with extrapolating clinically relevant information from a biomechanical setting. Cadaveric models are unable to precisely simulate an in vivo loading scenario and do not incorporate the factors of healing. It is possible that early callus formation may reinforce the fracture, thus minimizing the effects seen if encountering an additional load because of fall. However, compared with the in vivo setting, cadaveric radii may be more conducive for determining the appropriately matched VLP. The current findings were strengthened using a single-sex, matched-pair model to eliminate variability. This improved understanding within this homogenous sample. However, this model does limit the generalizability of the findings to other populations, including older adult females, who comprise the largest proportion of distal radius fractures. The experimental test setup was designed after a validated model of similar detail.[3] The use of a single implant limits the generalizability of the findings. Volar locked plates vary in design and in the quantity and trajectory of screws.

In conclusion, within the tested population sample, the current findings suggest that optimizing VLP width to the radial width may provide advantages for improved fragment capture and stability of the fixation construct.

Acknowledgments

The devices and specimens used for this work were provided through a material transfer agreement with Skeletal Dynamics, LLC. We thank Angelique Tapia, Rachel York, and A. Laurie Wells for editorial assistance.

References

1. Salibian AA, Bruckman KC, Bekisz JM, Mirrer J, Thanik VD, Hacquebord JH. Management of unstable distal radius fractures: a survey of hand surgeons. *J Wrist Surg*. 2019;8(4):335–343.
2. Orbay JL, Touhami A. Current concepts in volar fixed-angle fixation of unstable distal radius fractures. *Clin Orthop Relat Res*. 2006;445:58–67.
3. Salas C, Brantley JA, Clark J, Reda Taha M, Myers OB, Mercer D. Damage in a distal radius fracture model treated with locked volar plating after simulated postoperative loading. *J Hand Surg Am*. 2018;43(7):679.e1–679.e6.
4. Orbay JL. The treatment of unstable distal radius fractures with volar fixation. *Hand Surg*. 2000;5(2):103–112.
5. Obert L, Rey PB, Uhring J, et al. Fixation of distal radius fractures in adults: a review. *Orthop Traumatol Surg Res*. 2013;99(2):216–234.
6. Gutierréz-Espinoza H, Araya-Quintanilla F, Olguín-Huerta C, Gutiérrez-Monclus R, Jorquera-Aguilera R, Mathoulin C. Effectiveness of early versus delayed motion in patients with distal radius fracture treated with volar locking plate: a systematic review and meta-analysis. *Hand Surg Rehabil*. 2021;40(1):6–16.
7. Putnam MD, Meyer NJ, Nelson EW, Gesensway D, Lewis JL. Distal radial metaphyseal forces in an extrinsic grip model: implications for postfracture rehabilitation. *J Hand Surg Am*. 2000;25(3):469–475.
8. Kwon BC, Lee JK, Lee SY, Hwang JY, Seo JH. Morphometric variations in the volar aspect of the distal radius. *Clin Orthop Surg*. 2018;10(4):462–467.
9. Perrin M, Badre A, Suh N, Lalone EA. Analysis of three-dimensional anatomical variance and fit of the distal radius to current volar locking plate designs. *J Hand Surg Glob Online*. 2020;2(5):277–285.
10. Imatani J, Akita K. Volar distal radius anatomy applied to the treatment of distal radius fracture. *J Wrist Surg*. 2017;6(3):174–177.
11. Medoff RJ, Saucedo JM. Common errors of volar plate fixation. In: del Pinal F, Haerle M, Krimmer H, eds. *Distal Radius Fractures in Carpal Instabilities*. 1st ed. Thieme Medical Publishers; 2019:146–153.
12. Ma D, Schick B. Subchondral screw placement in volar plate fixation for distal radius fractures: a retrospective observational analysis. *J Hand Surg Eur Vol*. 2021;46(1):92–94.
13. Salas C, Neher L, Romero J, et al. Quantifying coverage of a distal radius volar plate using a novel pronator quadratus rotational muscle flap technique. *Western J Orthop*. 2020;9:74–77.
14. Shlaifer A, Atlan F, Kadar A, et al. Removal of volar plate after open reduction internal fixation of distal radius fractures: clinical and radiographic analysis. *Acta Orthop*. 2021;87:103–110.
15. Shaw JM, Hunter SA, Gayton JC, Boivin GP, Prayson MJ. Repeated freeze–thaw cycles do not alter the biomechanical properties of fibular allograft bone. *Clin Orthop Relat Res*. 2012;470(3):937–943.
16. Klein JS, Mijares MR, Chen D, Orbay JL, Landy DC, Owens PW. Radiographic evaluation of the distal radioulnar joint: technique to detect sigmoid notch intra-articular screw breach in distal radius fractures. *Tech Orthop*. 2020;35(1):73–77.
17. Schneider CA, Rasband WS, Eliceiri KW. NIH Image to ImageJ: 25 years of image analysis. *Nat Methods*. 2012;9(7):671–675.
18. Majima M, Horii E, Matsuki H, Hirata H, Genda E. Load transmission through the wrist in the extended position. *J Hand Surg Am*. 2008;33(2):182–188.
19. van Kampen RJ, Thoreson AR, Knutson NJ, Hale JE, Moran SL. Comparison of a new intramedullary scaffold to volar plating for treatment of distal radius fractures. *J Orthop Trauma*. 2013;27(9):535–541.
20. Konstantinidis L, Helwig P, Seifert J, et al. Internal fixation of dorsally comminuted fractures of the distal part of the radius: a biomechanical analysis of volar plate and intramedullary nail fracture stability. *Arch Orthop Trauma Surg*. 2011;131(11):1529–1537.
21. Blythe M, Stoffel K, Jarrett P, Kuster M. Volar versus dorsal locking plates with and without radial styloid locking plates for the fixation of dorsally comminuted distal radius fractures: a biomechanical study in cadavers. *J Hand Surg Am*. 2006;31(10):1587–1593.

22. Willis AA, Kutsumi K, Zobitz ME, Cooney WP III. Internal fixation of dorsally displaced fractures of the distal part of the radius. A biomechanical analysis of volar plate fracture stability. *J Bone Joint Surg Am*. 2006;88(11):2411–2417.
23. Rausch S, Klos K, Stephan H, et al. Evaluation of a polyaxial angle-stable volar plate in a distal radius C-fracture model—a biomechanical study. *Injury*. 2011;42(11):1248–1252.
24. Perren SM. Physical and biological aspects of fracture healing with special reference to internal fixation. *Clin Orthop Relat Res*. 1979;138(138):175–196.
25. Törnkvist H, Hearn TC, Schatzker J. The strength of plate fixation in relation to the number and spacing of bone screws. *J Orthop Trauma*. 1996;10(3):204–208.
26. Drobetz H, Schueller M, Tschegg EK, Heal C, Redl H, Muller R. Influence of screw diameter and number on reduction loss after plating of distal radius fractures. *ANZ J Surg*. 2011;81(1–2):46–51.
27. Wolfe SW, Swigart CR, Grauer J, Slade JF, Panjabi MM. Augmented external fixation of distal radius fractures: a biomechanical analysis. *J Hand Surg Am*. 1998;23(1):127–134.